THE JOURNAL OF PHYSICAL CHEMISTRY B

Article

pubs.acs.org/JPCB

Interactions of Sarin with Polyelectrolyte Membranes: A Molecular Dynamics Simulation Study

Ming-Tsung Lee, Aleksey Vishnyakov, Gennady Yu. Gor,[†] and Alexander V. Neimark*

Department of Chemical and Biochemical Engineering, Rutgers, The State University of New Jersey, 98 Brett Road, Piscataway, New Jersey 08854, United States

Supporting Information

ABSTRACT: Nanostructured polyelectrolyte membranes (PEMs), which are widely used as permselective diffusion barriers in fuel cell technologies and electrochemical processing, are considered as protective membranes suitable for blocking warfare toxins, including water-soluble nerve agents such as sarin. In this article, we examine the mechanisms of sorption and diffusion of sarin in hydrated PEMs by means of atomistic molecular dynamics simulations. Three PEMs are considered: Nafion, sulfonated polystyrene (sPS) that forms the hydrophilic subphase of segregated sPS−polyolefin block copolymers, and random sPS−polyethylene copolymer. We found that sarin concentrates at the interface between the hydrophilic and hydrophobic subphases of hydrated Nafion acting as a surfactant. In hydrated sPS, where the scale of water−polymer segregation is much smaller (1−2 nm), sarin also interacts favorably with hydrophobic and hydrophilic components. Water diffusion slows as the sarin content increases despite the overall increase in solvent content, which suggests that sarin and water have somewhat different pathways through the segregated membrane. Upon replacement of counterions of monovalent potassium with those of divalent calcium, sarin diffusion slows but remains substantial in all ionomers considered, especially at high sarin concentrations. The behavior of sarin is similar to that of its common simulant, dimethyl methylphosphonate.

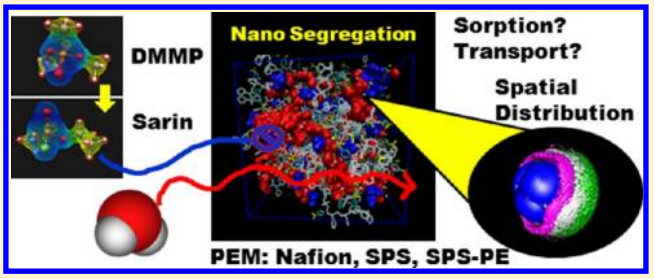

1. INTRODUCTION

Nanostructured polyelectrolyte membranes (PEMs) are widely used as permselective diffusion barriers in fuel cell technologies and electrochemical processing. PEMs are also considered as prospective components of breathable protective fabrics, suitable for blocking a wide variety of chemical warfare agents (CWAs), including water-soluble G-series nerve agents such as sarin (Figure 1a). Upon hydration, PEMs segregate into hydrophilic and hydrophobic subphases.[1,2] Ideally, water would diffuse through the hydrophilic subphase composed of water and ionic groups, whereas toxins, which contain a good share of hydrophobic groups, would be trapped in the hydrophobic subphase formed by the polymer backbone. However, experimental studies performed with the G-agent simulant dimethyl methylphosphonate (DMMP) in Nafion and sulfonated polystyrene (sPS) based block copolymers showed a limited applicability of this scenario.[3] First, DMMP readily sorbs in both Nafion and sPS−polyolefin block copolymers.[3,4] In Nafion DMMP diffusion is indeed slow at low hydration levels, but it becomes unacceptably fast as hydration increases. Replacing protons in PEMs with metal cations (especially with multivalent ions such as Ca^{2+}, Fe^{3+}, and Al^{3+}) helped slow DMMP transport, but DMMP diffusion in PEMs remained unacceptable at higher hydration.[3,5]

The sorption and transport properties of hydrated PEMs depend on the specifics of nanoscale segregation. Nafion (Figure 1b) is naturally segregated even in the dry state, as ionic side chains aggregate, forming small clusters. As water content increases, hydrophilic species form a continuous hydrophilic subphase. The scale of segregation varies but is believed to be on the order of several nanometers.[6] Segregation in sPS−polyolefin block copolymers differs fundamentally, because its scale is proportional to the block length and is much larger than in Nafion. Comparison of DMMP sorption in sPS−PB−sPS (PB = polybutadiene) triblock copolymers and pure PB showed that DMMP is mainly sorbed within the hydrophilic subphase.[4] Both experiments and simulations suggest that the hydrophilic subphase is also strongly heterogeneous on the scale of about 2 nm.[7,8]

Because of the extreme toxicity of G agents, experiments are performed almost exclusively with simulant compounds of lower toxicity that have chemical structures and molecular sizes similar to those of the CWAs of interest. Because of the apparent difficulty of experimental studies, molecular modeling becomes a natural choice for exploring the mechanisms of sorption and diffusion of G agents and their simulants in PEMs.[8−12] Modeling of agents and simulants in similar environments could also verify whether simulants accurately mimic behavior of their corresponding CWA, which was recently questioned, in particular for perfluorinated polymers.[11]

Received: September 6, 2012
Revised: November 30, 2012
Published: December 3, 2012

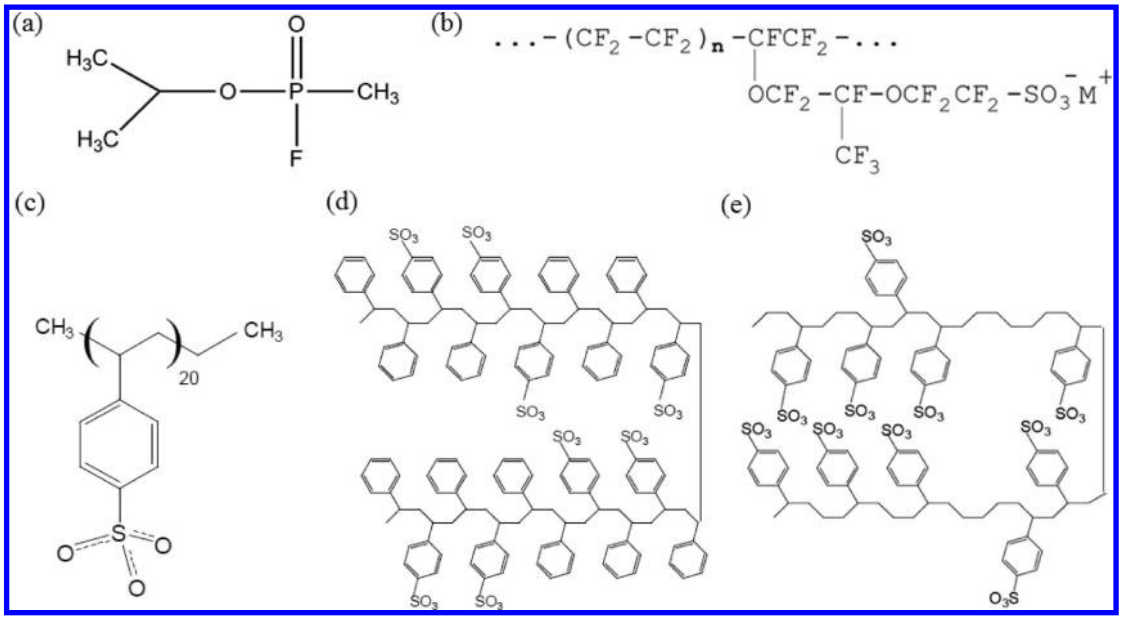

Figure 1. Atomic structures of the molecules used in this work: (a) sarin; (b) Nafion, n = 7, counterion M is K^+ or Ca^{2+} in this work; (c) 100% sulfonated polystyrene fragment; (d) 40% sulfonated polystyrene fragment; and (e) pseudorandom sulfonated ethylene−styrene copolymer.

In this article, we employ molecular dynamics (MD) simulations to study the behavior of sarin in dry and hydrated sPS, random sPS−PE block copolymers (PE = polyethylene), and Nafion, which serves as a reference system. Section 2 describes the models, methods, and simulation details. In section 3, we fit some of the parameters of a second-order empirical force field for Nafion to our ab initio calculations. In sections 4 and 5, we describe the results of our molecular dynamics simulations and discuss the mechanisms of sorption and transport of sarin in Nafion and sPS. Section 6 contains a discussion of perspectives on the application of PEMs as barrier materials.

2. MODELS AND METHODS

In MD simulations Nafion was represented by four-unit oligomers. The monomer is shown in Figure 1b. n was set to 7, which corresponds to the equivalent polymer weight of 1163 in acid form. sPS was represented by short fragments of tactic PS composed of 20 monomers, some of which were sulfonated at para positions. These oligomers were described previously.[10] We studied sPS samples at two sulfonation levels, namely, 100% (sulfonate groups attached to all phenyl rings) and 40%, with sulfonate groups attached to 8 of 20 benzene rings (Figure 1c,d), as well as one sample of random sPS−PE copolymer depicted in Figure 1e. The counterions, K^+ and Ca^{2+}, were modeled as charged Lennard-Jones spheres.[13,14]

The simulation procedures were similar to those employed in refs 10, 15, and 16. We used the MDynaMix[17] software package. The oligomers, counterions, and solvent molecules were placed in a cubic box at very low density. Additional details are given in the Supporting Information, section S2. The system was then gradually contracted in a series of constant-temperature MD simulations at T = 303 K maintained by a simple velocity scaling. After the density of 1.0 g/cm^3 (sPS) or 1.7 g/cm^3 (Nafion) was achieved, the simulation proceeded at P = 1 atm and T = 303 K maintained with the Nosé−Hoover thermostat.[18,19] System equilibration was performed for 2−6 ns, followed by an additional 10−20 ns of MD simulation, over which the system configuration was periodically saved for further analysis. It is worth noting that, although the Monte Carlo (MC) insertion of solvent molecules into the polymer matrix would be the best approach to mimic the experimental conditions of solvent sorption, a low probability of insertions into a dense glassy polymer makes this approach computationally expensive. The method of gradual contraction of the system in NPT MD simulation that we applied represents a reasonable approach to obtain configurations close to equilibrium. During NPT MD simulation runs, we monitored the segregation process computing the variations of energy and volume, as well as the number of hydrogen bonds between water molecules. It appeared that the segregation structure did not change appreciably after the first 5 ns of the NPT MD trajectory. The simulations of Nafion and other electrolytes published in the literature suggest that the time scale of several nanoseconds is reasonable for studying the segregation and self-diffusion of the solvents[20−23] in an essentially static polymeric matrix.

For sPS fragments, we employed the second-order classical force field that we constructed in ref 10. It is based on the TraPPE force field of Wick et al.[24] with parameters for sulfonate groups fitted to the results of restricted Hartree−Fock (RHF)/density functional theory (DFT) minimization.[10] A force field for Nafion is described in the next section. Water was presented by the simple-point-charge (SPC) model,[25] and sarin was modeled by the model of Sokkalingam et al.[26] All sarin molecules were R stereoisomers, as in our previous ab initio calculation study,[11] which is consistent to the lowest-energy conformation at the level of second-order Møller−Plesset perturbation theory in the work by Kaczmarek et al.[27] The Newton equations of motion were integrated using the standard Verlet algorithm with a double time step of 0.2 fs for rapidly fluctuating forces and 2.0 fs for other forces.[28] Long-range electrostatic forces were calculated using the Ewald summation.

3. NAFION FORCE FIELD

Following the work of Urata et al.,[29] we used the parameters from refs 30−33 for the perfluoroether skeleton and side chain and Lennard-Jones parameters for the sulfonate groups, as in

dx.doi.org/10.1021/jp308884r | J. Phys. Chem. B 2013, 117, 365−372

Table 1. Systems and Physical Properties

polymer[a]	solvent content (water, sarin) b	c	density (g/cm^3)	D_{ion}	D_{H_2O} (10^{-9} m^2/s)	D_{sarin}	D_{H_2O}/D_{sarin}[d]	n_{HB}[e] – H_2O	n_{HB}[e] – sarin	ratios of n_{HB}[f] – H_2O, –sarin	n_{HB}[e] $-SO_3$	n_{HB}[e] total
Nafion, K^+	0, 30	–	1.80	g	–	0.020	–	–	–	–	–	–
sPS, 100%, K^+	0, 30	–	1.30	g	–	g	–	–	–	–	–	–
sPS–PE, 100%, K^+	0, 30	–	1.23	g	–	g	–	–	–	–	–	–
sPS, 40%, K^+	0, 30	–	1.20	g	–	g	–	–	–	–	–	–
Nafion, K^+	10, 10	0.89, 0.11	1.88	0.020[h]	0.075[h]	0.020[h]	4	1.03	0.15	0.87, 0.13	0.80	1.97
sPS, 100%, K^+	10, 10	0.89, 0.11	1.34	g	0.0070	g	7	0.34	0.05	0.87, 0.13	1.48	1.87
sPS–PE, 100%, K^+	10, 10	0.89, 0.11	1.26	g	0.0094	g	10	0.40	0.07	0.85, 0.15	1.34	1.81
sPS, 40%, K^+	10, 10	0.89, 0.11	1.22	g	0.012	g	8	0.51	0.07	0.88, 0.12	1.29	1.87
sPS, 40%, K^+	30, 10	0.96, 0.04	1.21	0.023	0.14	0.004	34	1.12	0.05	0.96, 0.04	0.77	1.94
sPS, 40%, K^+	54, 10	0.98, 0.02	1.19	0.18	0.46	0.010	45	1.42	0.04	0.97, 0.03	0.53	1.99
sPS, 40%, K^+	54, 50	0.89, 0.04	1.18	0.023	0.34	0.14	2	1.37	0.16	0.90, 0.10	0.53	2.06
sPS, 40%, Ca^+	54, 10	0.98, 0.02	1.17	0.001[g]	0.26	0.004	69	1.53	0.03	0.98, 0.02	0.38	1.94

[a]Skeleton chemical structures as shown in Figure 1, sulfonation level, and modified counterion. [b]Solvent content in terms of weight percentage of dry polymer. [c]Solvent content in terms of molar fraction of solvent (water and sarin only). [d]Ratio of water self-diffusion coefficient to sarin diffusion coefficient. [e]Number of hydrogen bonds donated by one water molecule. A hydrogen bond is considered using the criteria that the bond length is less than 3.4 Å and the OHO angle exceeds 120°. [f]Ratio of numbers of hydrogen bonds between two water molecules and between water and sarin. [g]Mean square displacement too small to determine diffusion coefficient. [h]System size comparable to segregation scale and insufficient to accurately describe diffusion in hydrated Nafion.

our previous simulations.[8,20] The other parameters were fitted to the results of ab initio calculations performed at the B3LYP/cc-pvdz level of theory; the basis set was chosen following ref 33. Calculations were performed using the PQS Ab Initio software package.[34,35]

The following molecules were considered and the corresponding parameters extracted: $CF_3SO_3^-$ (C–S and S=O stretching, C–S–O and O–S–O angle bending), CF_3–O–CF_2–CF_2–O–CF_3 (O–CF_x–CF_x–O dihedral), CF_3–O–CF_2–CF_2–SO_3^- (O–CF_x–CF_x–S dihedrals). The equilibrium distances and angles as well as rigidities were calculated by scanning the energies along the corresponding variables. To obtain the potential functions for the dihedral angles, we optimized each molecule at fixed dihedral angle and then deducted electrostatic, Lennard-Jones, angle-bending, and bond-stretching contributions. The difference was attributed to the dihedral energy to achieve the best fit of the classical force field energies to the ab initio energies. In Nafion, the 1–4 nonbonded interactions were not taken into account, but all 1–5 nonbonded interactions were; however, we used a "special" zero interaction between the ether and sulfonate oxygens in the –O–CF_2–CF_2–SO_3^- fragment. The Supporting Information contains a table of Nafion parameters; the energy profiles associated with variation of bonds, angles, and torsions of the reference molecules; and the profiles of the torsion terms of the force field.

4. SORPTION AND DIFFUSION OF SARIN IN DRY AND HYDRATED NAFION

Segregation in hydrated Nafion has been a subject of numerous experimental, theoretical, and simulation studies (see reviews).[10,36−39] Large-scale simulations of Nafion performed by coarse-grained MD and dissipative particle dynamics (DPD) allowed studies of segregation morphology and comparison with the experiments. Hayes et al.[40] built a unified picture of hydrated Nafion segregation merging simulation and experimental results. In general, the simulation scale needs to substantially exceed the segregation scale and to include at least several water aggregates. In this article, we aim not at studying the segregation morphology of Nafion in the presence of sarin, but rather at revealing the mechanisms of sarin sorption on the atomistic scale. This stage is necessary for further modeling of the effects of sarin sorption on PEM segregated morphology and its diffusive penetration through the membrane.

Experiments with DMMP[3] show that Nafion is capable of sorbing large amounts of phosphororganic compounds. When considering dry polymer, the sarin concentration was set to 30% of the dry polymer weight, which (if the DMMP results can be projected to sarin) would correspond to the sarin vapor partial pressure of 111.1 Pa at room temperature.[41] We should note that this is not a realistic situation because, under environmental conditions, the membrane is always hydrated to some extent. However, this system helps focus on sarin–polymer interactions unaffected by water. In hydrated Nafion, the water content was set at 10 wt %, which corresponds to approximately 90% humidity in K^+-substituted Nafion, and the sarin content was set also at 10 wt %, so that the qualitative results could also be projected to low sarin concentrations. The entire list of the systems studied is given in Table 1.

Figure 2 shows snapshots of Nafion skeleton and sarin in dry and hydrated Nafion. It is quite clear that, when solvated with sarin, Nafion undergoes segregation into a backbone subphase and a sarin subphase. At 30 wt % (Nafion is able to sorb up to 120–140 wt %[3,5] DMMP, and maximum sorption of sarin is expected to be on the same order of magnitude), it is clear that sarin forms a continuous subphase. The clusters of sulfonate groups, which appear relatively tight in comparison with those in hydrated Nafion, are surrounded by sarin, as confirmed by the radial distribution functions (RDFs) $g_{AB}(r)$, calculated as the average concentration of A atoms around a B atom at a distance r related to the average concentration of B atoms in the system (Figure 3a,b). As water is added, the situation qualitatively changes, as seen from the snapshots in Figure 2 and quantified by the RDFs in Figure 3c,d. Specifically, the

dx.doi.org/10.1021/jp308884r | J. Phys. Chem. B 2013, 117, 365−372

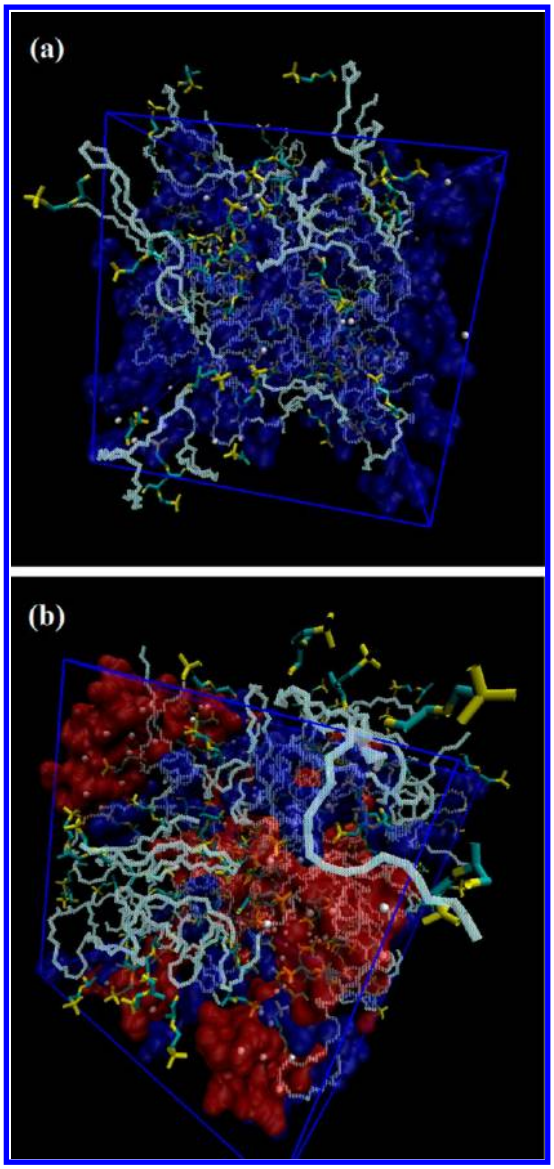

Figure 2. Snapshots of Nafion fragments in (a) 30 wt % sarin (solvent surface shown in blue) and (b) 10 wt % sarin and 10 wt % water (solvent surface shown in red). Nafion backbones are drawn in white, and side chains are marked in green (perfluoroether) and yellow (sulfonate groups). Dots represent potassium counterions. Box length: (a) 51.3 and (b) 50.7 Å.

sulfonate groups are surrounded by water, as the first peak of the RDF for sulfur and water oxygens is much higher than that for sulfur and sarin oxygens. At the same time, there is a broad and very prominent peak in the RDF between the phosphorus atoms of sarin and the perfluoroether oxygens of Nafion side chains (Figure 3d), which shows that the sarin local concentration is higher around the ether oxygen near the sulfonate group (OC7) rather than that near the backbone (OC11). Altogether, it is clear that sarin is not dissolved in the fluoroalkane backbone but rather is concentrated around the middle perfluoroether segment of the side chains, which agrees with pulse-gradient NMR results obtained by Giotto et al.[42] for DMMP.[5] This behavior stems not from very favorable interactions between side chains and sarin, but rather from the chemical structure of these phosphororganic compounds that contain strongly hydrophilic and strongly hydrophobic segments: The sarin "head" interacts with water and counterions, but the hydrocarbon "tail" interacts with the fluorocarbon backbone at the same time. Geometric analysis showed that, at 10 wt % water and 10 wt % sarin, water consistently forms a continuous subphase. Sarin does not necessarily form a continuous subphase; small inclusions consisting of single or several sarin molecules are often trapped between aqueous and organic subphases. The organic backbone, of course, does form a continuous subphase. It is typically possible to distinguish three continuous regions (Figure 2b): (i) fluorocarbon backbone; (ii) sarin and perfluoroether side chain; and (iii) water, counterions, and sulfonate ions.

A distinct sarin subphase in dry Nafion seems to mean facile transport, but in fact, this might not be the case. First, the simulation size available for atomistic MD is not sufficient to examine the connectivity of the sarin subphase and the diffusion coefficient. Both experiments[43−45] and simulations[16] show that DMMP is a strong deplasticizer, which makes the polymer skeleton very rigid. The sarin molecule is about 8 times larger than the water molecule; it effectively has to diffuse in a network of very narrow pores that are one to two sorbate molecules in diameter and have rough walls. Diffusion in such pores could easily be a few orders of magnitude slower than that in bulk system and effectively negligible.[8] However, in hydrated Nafion, sarin molecules are located at the interface between the subphases and are surrounded by much more mobile water molecules. This enables a facile diffusion of sarin in the surface layer.

Using the Einstein equation for diffusion in two dimensions, $D_{\|} = \mathrm{d}/\mathrm{d}t\langle {}^1/_4[r(t) - r(t_0)]^2\rangle$, we estimated the in-plane diffusion coefficient of sarin placed on a Nafion film and surrounded by water. The mobility of sarin is dominated by in-plane diffusion rather than sorption−desorption of sarin molecules and transport in the surrounding water. The mean square displacement (MSD) of solvent in the lateral direction was recorded within the time interval of 10−15 ns. The film area was 3 × 3 nm, the thickness was ca. 2 nm, and the total system size in the normal direction was about 5 nm. The diffusion coefficient was close to 1×10^{-10} m^2/s, which is only about one-fourth of the water in-plane self-diffusion coefficient in the layer close to the Nafion−water interface. It is unacceptably fast because the permselectivity of PEMs is achieved by the differences in diffusion coefficients of water and sarin.

5. SORPTION AND DIFFUSION OF SARIN IN HYDRATED SPS

Following our previous work,[8,10] we considered sPS with 40% of benzene rings sulfonated, all in the para position. This sulfonation level was chosen by Schneider et al. in their studies of DMMP in sPS-based block copolymers.[3,4] In the sPS system with 40% sulfonation, we considered different water contents from 0% to 54% of the dry sPS weight. The limit of 54% was derived from the experimental data on water sorption in sulfonated PS−(PE−PB)−PS triblock copolymer membranes with the same counterion, assuming that water sorption in the hydrophobic phase is negligible.[4] The sarin content was varied from 10 to 50 wt %. In addition, 100% sulfonated sPS and pseudorandom 100% sulfonated PS−PE copolymer were modeled for comparison.

Figure 4 shows snapshots of configurations containing 40% sPS, sarin, and water at three different solvent compositions. Geometric analysis shows that, at a water content of 10 wt %,

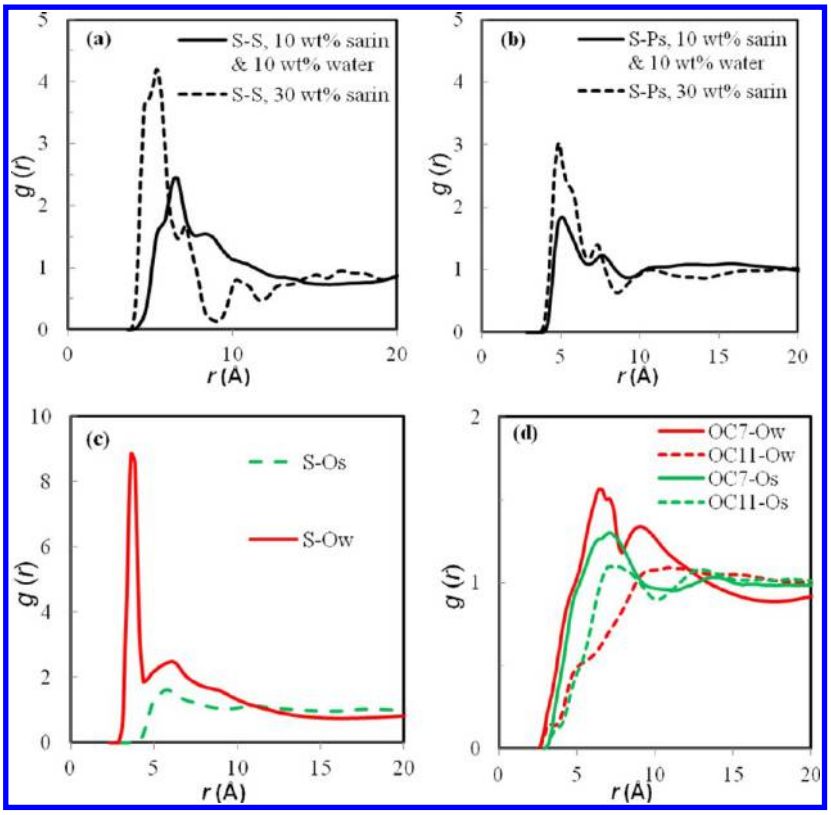

Figure 3. Radial distribution functions of dry Nafion fragments with 30 wt % sarin (dashed lines) and hydrated Nafion fragments with 10 wt % water and 10 wt % sarin (solid lines). (a) Intermolecular RDFs of sulfur atoms on Nafion sulfonate groups. (b) RDFs of sulfur atom with sarin phosphorus. (c) RDFs of sulfur atom with sarin oxygen (P═O, green dashed line) and water oxygen (red solid line). (d) RDFs of ether oxygens on two locations of the Nafion side chain with sarin oxygen Os (green lines) and water oxygen Ow (red lines). OC7 (solid lines) is located near the sulfonate group, and OC11 (dashed lines) is located near the backbone. The first peaks of the OC7 RDFs show the competition between water and sarin around sulfonate groups. The OC11 RDFs show that sarin prefers the ether oxygen but water shows low preferences because of its repeal of the backbone. All RDFs together reveal that sarin's attractions to sulfonate groups are similar to those of water and that it has an amphiphilic nature.

there is a continuous water path through the polymer. At higher solvent contents, the system is microsegregated, and one can distinguish continuous subphases formed by polymer backbone and solvents. Of course, a strong nonuniformity is expected in the system, with two components composed of both hydrophilic and hydrophobic groups separated by considerable distances. To characterize the local structure, we calculated the number of hydrogen bonds (H-bonds) in all sPS systems using simple geometric criteria: A H-bond was considered to be "established" when two oxygens were found at a distance of less than 3.3 Å with an OHO angle exceeding 120°.[46,47] Note that a hydrogen-bonding term was not included in the force field. The effective H-bonds defined by geometric criteria resulted from electrostatic and van der Waals interactions, and the number of effective H-bonds simply characterizes the geometric arrangement of molecules. Because only water donates hydrogen bonds in the systems considered, there is always an excess of acceptors, including water, sulfonate oxygens, and sarin oxygens connected to their phosphorus atoms by double bonds (the other sarin oxygen and fluorine atoms show a very weak tendency to form H-bonds). In all of the systems, the total number of H-bonds donated per water molecule is very close to the full capacity of 2. In our ab initio and MD study of water−sarin hydrogen bonding, we observed that sarin oxygens are about as attractive as acceptors as water oxygens.[11,12] From Table 1, one can see that the ratio of water−water to water−sarin H-bonds is very close to the molar ratio between the two solvents, except in the most hydrated systems, but even in those cases, they do not deviate considerably. This means that sarin oxygens are well exposed to water and that segregation is mostly limited to two molecular layers.

Table 1 also lists the self-diffusion coefficients of both solvents and counterions calculated with the Einstein equation (see the Supporting Information for an example and details). Interestingly, the experimentally measured water diffusion at comparable water content but lower sulfonation[48] is dramatically slower than in our simulations. For example, Li^+-modified sPS at a 3.6% sulfonation level sorbs 6.4 wt % water with $D = 0.2 \times 10^{-13}$ m^2/s. We explain this difference as resulting from a different nanostructure at lower sulfonation levels: Water forms isolated aggregates around sulfonate groups rather than a continuous network. To verify our model, we also considered 5% sulfonated, Li^+-substituted sPS at 7 wt % water content. We observed isolated water aggregates and were unable to determine the diffusion coefficient. Thus, the hydrophilic subphase is below percolation in that system, which qualitatively agrees with experimental data. We also examined experimental data for sulfonated polyethersulfone membranes.[49] Our values are of the same order of magnitude, but a direct comparison is not possible, because the polymer chemistry is different between the two systems.

The systems in Table 1 are formed by a relatively immobile polymer and three mobile species, namely, solvents and counterions. One might expect the diffusion of the mobile components to become faster as the amount of sorbed solvent increases. This is generally true. For example, the water

dx.doi.org/10.1021/jp308884r | J. Phys. Chem. B 2013, 117, 365−372

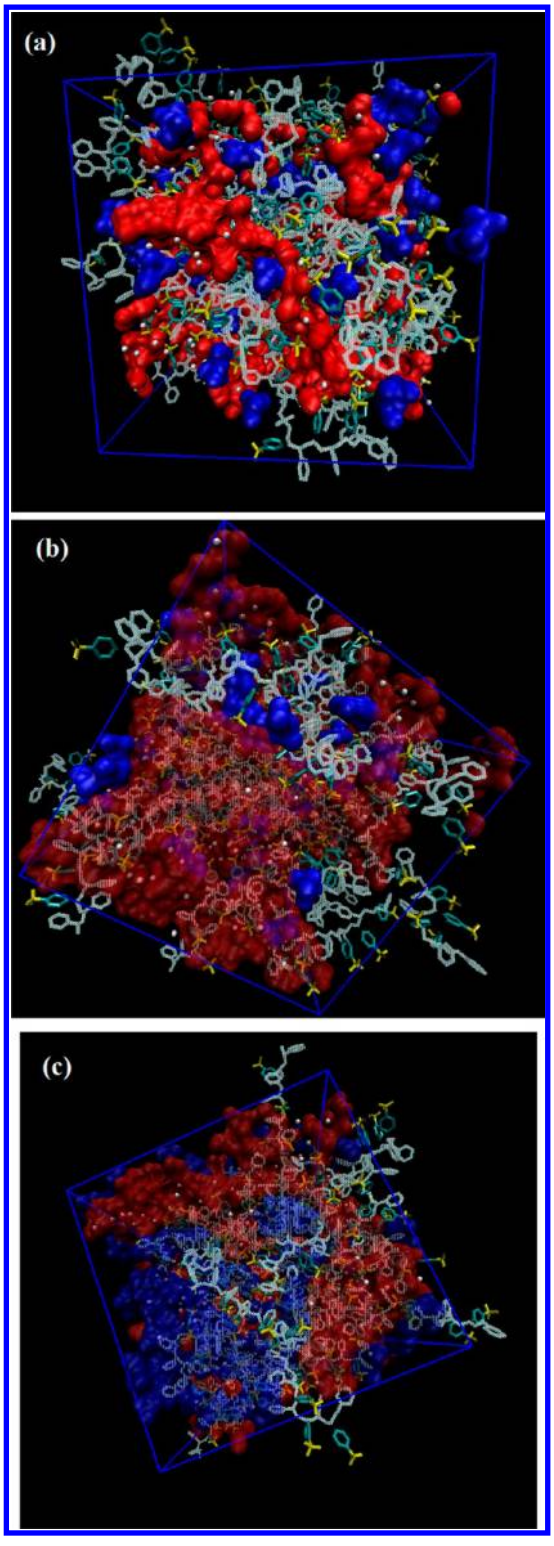

Figure 4. Snapshots of 40% sulfonated polystyrene fragments in (a) 10 wt % sarin (solvent surface shown in red) and 10 wt % water (solvent surface shown in blue), (b) 10 wt % sarin and 54 wt % water, and (c) 50 wt % sarin and 50 wt % water. Hydrophobic backbones of polymer fragments are drawn in white, and side chains are marked in green (sulfonated benzene rings) and yellow (sulfonate groups). Dots represent potassium counterions. Box length: (a) 54.5, (b) 54.6, and (c) 54.5 Å.

diffusion coefficient increases by more than an order of magnitude as the water amount increases from 10 to 30 wt % in the K^+ form of 40% sulfonated PS, and the diffusion achieves nearly 21% of the bulk water diffusion coefficient as the water sorption increases to 54 wt % (and the sarin content remains constant at 10 wt %). Sarin diffusion also becomes faster but at a much lower pace: The ratio of water and sarin diffusion coefficients is about 7−10 at 10 wt % sarin and 10 wt % water and increases to about 45 at 10 wt % sarin and 54 wt % water. If the sarin content increases from 10 to 50 wt %, the water diffusion coefficient decreases slightly, whereas the sarin diffusion coefficient increases by a factor of 13 and is only about one-third of the bulk sarin value. A geometric analysis of the segregation structure shows that sarin essentially forms a continuous subphase of its own, in which it can diffuse even if it does not mix with water, as shown in Figure 4c.

The diffusion coefficients obtained suggest that sarin and water diffuse in somewhat different environments. Geometric analysis shows that as sarin concentrates around the polystyrene backbone with hydrophilic heads exposed to water, somewhat similarly to the sulfonate groups. Figure 5

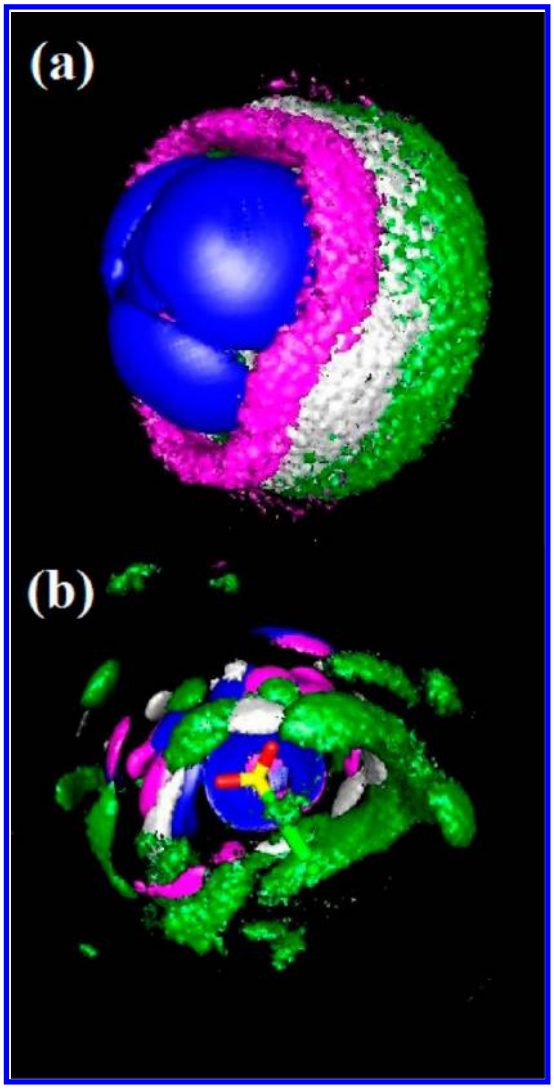

Figure 5. Spatial distribution functions for water oxygen (dark blue), phosphorus (gray), O(═P) oxygen (purple), and CH carbons of sarin (green) around the phenylsulfonate side chain of the sPS with (a) K^+ and (b) Ca^{2+} counterions. The intensity levels are as follows: (a) O_w, 4; O_P, 3, P, 3.2; CH, 2.5; (b) O_w, 10; O_P, 7; P, 7; CH, 5.

dx.doi.org/10.1021/jp308884r | J. Phys. Chem. B 2013, 117, 365−372

shows the spatial distribution functions (three-dimensional density profiles calculated in a reference coordinate system rigidly attached to a part of the molecule of interest) for several different solvent atoms around the phenylsulfonate side chain. Here, the local coordinate system is attached to the relatively rigid sulfonate group. The positions of each side chain and the surrounding solvent atoms are recorded with respect to this coordinate system. Then, these positions are converted into local densities. The colored clouds show the areas where the probability of finding an atom of a particular kind exceeds the average by a certain factor. The average positions of the benzene ring all fall onto the axis because of rotation of the sulfonate group. As expected, water oxygens are located near the sulfonate oxygens, to which they donate H-bonds, whereas sarin is located around the benzene ring, and the farther the atom is from the tail methyl groups, the closer its cloud is to sulfonate oxygens. This means that sarin is generally oriented parallel to the side chains, like a small surfactant: Its tail is protruded into the alkane skeleton, and its head is protruded into water. As the sarin concentration increases, water interacts with the hydrophilic heads of sarin molecules, whose mobility is restricted by their larger size and phenyl groups. Because the components do not really mix in the sPS environment, the volume fraction effectively available for water diffusion does not increase, whereas interactions with the environment become stronger, thus reducing the water mobility. One might notice the water and sarin segregation shown in Figures 2 and 4, which is consistent with our previous MD simulation of sarin and water mixtures,[12] and it can be explained by a recent ab initio study of sarin microhydration by Alam et al.,[50] in which the adsorption free energies of sarin were examined with multiple water molecules.

Interestingly, this apparent scenario does not exactly apply if the counterion is changed to divalent calcium Ca^{2+}. The Ca^{2+}−S RDF shows that all counterions are associated with at least one sulfonate group and about 20% of counterions are associated with two sulfonate groups. As a result of uncompensated charges, the solvent structuring around the sulfonate group is much more distinct, with certain preferential positions of sarin oxygens around the sulfonate group, despite their inability to form a hydrogen bond. The structuring and "cross-linking" of the side chains by counterions slow the diffusion in the system. Sarin diffusion in Ca^{2+}-substituted sPS slows faster than that of water, as the ratio of self-diffusion coefficients drops to 1/69 from 1/45, which was observed in K^+-substituted sPS. Chain cross-linking by divalent Ca^{2+} is visible from the number of water molecules in the first hydration shell of the ion. Based on literature ab initio studies for K^+ and Ca^{2+} bulk hydration, Ca^{2+} can coordinate up to eight water molecules in the first solvation shell,[51,52] and the hydration number for K^+ is reported as 6.[53] The estimated hydration numbers from the first solvation shell in the radial distribution function of water oxygen with K^+ and Ca^{2+} are 6.6 and 3.5. The trend opposite to that of the bulk shows the strong association between divalent calcium ions and sulfonate groups.

6. CONCLUSIONS

In this work, we studied the mechanisms of sorption and transport of the phosphororganic agent sarin in two dry and hydrated polyelectrolytes, namely, Nafion and sufonated polystyrene that forms the hydrophilic subphase of sPS−polyolefin block ionomers, considered as prospective protective barrier materials. The specifics of the sorption and transport in this system are determined by (1) the "Janus-like" structure of the sarin molecule, which has both strongly hydrophobic and strongly hydrophilic fragments, as is typical for phosphor-organic CWAs, and (2) the nanostructure of polyelectrolytes that are segregated into hydrophilic and hydrophobic regions. As a result, sarin interacts favorably with both the hydrophobic and hydrophilic content of hydrated membranes. In Nafion, where the segregation is well-defined and its scale reaches 4−5 nm, sarin was observed to concentrate at the interface between the hydrophobic subphase formed by the perfluorocarbon backbone and the hydrophilic subphase of water and counterions. Here, sarin effectively behaves like a surfactant. Its proximity to water clusters facilitates sarin diffusion in Nafion along the subphase interfaces. The interfacial mechanism of sarin diffusion appears to dominate diffusion through the aqueous or organic subphase, where sarin does not seem to get trapped, contrary to the scenario desirable from the practical viewpoint.

In sPS−polyolefin block copolymers, the transport of both phosphororganic agents and water has to occur through the same (hydrophilic) subphase of hydrated sPS. The sPS itself segregates on a substantially smaller scale of 1−2 nm and is far less distinct than in Nafion. As such, the concept of trapping phosphororganic agents by hydrophobic polymer backbone seems to work, as the agent is "wrapped" along the phenylsulfonate (or just phenyl) side chains. Still, it appears that the desired ratio between the water and agent diffusivities is unlikely to be reached even at relatively low agent contents. If its content increases to about 50% of the dry polymer weight, the agent essentially forms a continuous subphase of its own inside the hydrophilic subphase, and its diffusion becomes unreasonably fast. Note that 50% is surely lower than the full sorption capacity of sPS toward the agent.

Replacing monovalent potassium with divalent calcium would certainly improve the membrane blocking properties against sarin through local structuring of the solvent around the ions and sulfonate group cross-linking. Apparently, ions that are able to chemically form complexes with water and agents, such as Ca^{2+} or Fe^{3+},[5] will further decrease agent penetration. Nevertheless, it appears to us that the blocking performance of PEMs can be improved using highly chemically cross-linked polyelectrolytes with less hydrophobic composition. Chemical cross-linking should reduce the general sorption capacity of PEMs, and a strongly hydrophilic environment should change the mechanism of sorption of Janus-like molecules of phosphororganic agents and make it more similar to the mechanism of water sorption. Sorption in PEMs needs to be selective toward water rather than the semicooperative sorption observed currently.

Finally, a comparison of our results with those published previously on DMMP shows that alkylphosphonates mimic the behavior of G agents in segregating polyelectrolytes reasonably well, on a semiquantitative level. It should also be noted that the segregation behavior of sarin in hydrated polyelectrolytes with simple cations is determined by nonspecific hydrophilic−hydrophobic interactions. This is why one can expect that other compounds that are completely different from phosphororganic agents in their chemistry but contain both strongly hydrophilic and strongly hydrophobic groups separated by a considerable distance would have mechanisms of sorption and transport in polyelectrolytes similar to those observed for sarin in this work.

dx.doi.org/10.1021/jp308884r | J. Phys. Chem. B 2013, 117, 365−372

■ ASSOCIATED CONTENT

Supporting Information

Modified parameters of the Nafion force field and calculation details (section S1), details of MD simulations that did not fit into Table 1 (section S2), examples of self-diffusion coefficient calculations and molecule displacement distribution (section S3), and ion−water RDFs (section S4). This material is available free of charge via the Internet at http://pubs.acs.org.

■ AUTHOR INFORMATION

Corresponding Author

*E-mail: aneimark@rci.rutgers.edu.

Present Address

[†]Department of Civil and Environmental Engineering, Princeton University, E228 Engineering Quadrangle, Princeton, NJ 08544. E-mail: ggor@princeton.edu.

Notes

The authors declare no competing financial interest.

■ ACKNOWLEDGMENTS

This work was supported by DTRA Grant HDTRA1-08-1-0042 “Multiscale Modeling of Permeability of Protective Polyelectrolyte Membranes to CBW Agents”.

■ REFERENCES

(1) Won, J.; Choi, S. W.; Kang, Y. S.; Ha, H. Y.; Oh, I. H.; Kim, H. S.; Kim, K. T.; Jo, W. H. *J. Membr. Sci.* **2003**, *214*, 245−257.
(2) Kim, B.; Kim, J.; Jung, B. *J. Membr. Sci.* **2005**, *250*, 175−182.
(3) Schneider, N. S.; Rivin, D. *Polymer* **2004**, *45*, 6309−6320.
(4) Schneider, N. S.; Rivin, D. *Polymer* **2006**, *47*, 3119−3131.
(5) Rivin, D.; Meermeier, G.; Schneider, N. S.; Vishnyakov, A.; Neimark, A. V. *J. Phys. Chem. B* **2004**, *108*, 8900−8909.
(6) Eisenberg, A., Yeager, H. L., Eds. *Perfluorinated Ionomer Membranes*; American Chemical Society: Washington, DC, 1982; Vol. *180*.
(7) Gromadzki, D.; Cernoch, P.; Janata, M.; Kudela, V.; Nallet, F.; Diat, O.; Stepanek, P. *Eur. Polym. J.* **2006**, *42*, 2486−2496.
(8) Vishnyakov, A.; Neimark, A. V. *J. Phys. Chem. B* **2008**, *112*, 14905−14910.
(9) Vishnyakov, A.; Neimark, A. V. *J. Phys. Chem. A* **2004**, *108*, 1435−1439.
(10) Vishnyakov, A.; Neimark, A. V. *J. Chem. Phys.* **2008**, *128*, 164902.
(11) Lee, M.-T.; Vishnyakov, A.; Gor, G. Y.; Neimark, A. V. *J. Phys. Chem. B* **2011**, *115*, 13617−13623.
(12) Vishnyakov, A.; Gor, G. Y.; Lee, M.-T.; Neimark, A. V. *J. Phys. Chem. A* **2011**, *115*, 5201−5209.
(13) Heinzinger, K. *Physica B* **1985**, *131*, 196−216.
(14) Marchand, S.; Roux, B. *Biophys. J.* **1996**, *70*, SUAM4−SUAM4.
(15) Vishnyakov, A.; Neimark, A. V. *J. Phys. Chem. B* **2000**, *104*, 4471−4478.
(16) Vishnyakov, A.; Neimark, A. V. *J. Phys. Chem. B* **2001**, *105*, 7830−7834.
(17) Lyubartsev, A. P.; Laaksonen, A. *Comput. Phys. Commun.* **2000**, *128*, 565−589.
(18) Hoover, W. G. *Phys. Rev. A* **1985**, *31*, 1695−1697.
(19) Nose, S. *J. Chem. Phys.* **1984**, *81*, 511−519.
(20) Vishnyakov, A.; Neimark, A. V. *J. Phys. Chem. B* **2001**, *105*, 9586−9594.
(21) Jang, S. S.; Lin, S. T.; Cagin, T.; Molinero, V.; Goddard, W. A. *J. Phys. Chem. B* **2005**, *109*, 10154−10167.
(22) Jang, S. S.; Goddard, W. A. *J. Phys. Chem. C* **2007**, *111*, 2759−2769.
(23) Cui, S. T.; Liu, J. W.; Selvan, M. E.; Keffer, D. J.; Edwards, B. J.; Steele, W. V. *J. Phys. Chem. B* **2007**, *111*, 2208−2218.
(24) Wick, C. D.; Martin, M. G.; Siepmann, J. I. *J. Phys. Chem. B* **2000**, *104*, 8008−8016.
(25) Berendsen, H. J. C.; Grigera, J. R.; Straatsma, T. P. *J. Phys. Chem.* **1987**, *91*, 6269−6271.
(26) Sokkalingam, N.; Kamath, G.; Coscione, M.; Potoff, J. J. *J. Phys. Chem. B* **2009**, *113*, 10292−10297.
(27) Kaczmarek, A.; Gorb, L.; Sadlej, A. J.; Leszczynski, J. *Struct. Chem.* **2004**, *15*, 517−525.
(28) Tuckerman, M. *J. Chem. Phys.* **1992**, *97*, 1990.
(29) Urata, S.; Irisawa, J.; Takada, A.; Shinoda, W.; Tsuzuki, S.; Mikami, M. *J. Phys. Chem. B* **2005**, *109*, 4269−4278.
(30) Cui, S. T.; Cochran, H. D.; Cummings, P. T. *J. Phys. Chem. B* **1999**, *103*, 4485−4491.
(31) Cui, S. T.; Siepmann, J. I.; Cochran, H. D.; Cummings, P. T. *Fluid Phase Equilib.* **1998**, *146*, 51−61.
(32) Li, H. C.; McCabe, C.; Cui, S. T.; Cummings, P. T.; Cochran, H. D. *Mol. Phys.* **2002**, *100*, 265−272.
(33) Li, H. C.; McCabe, C.; Cui, S. T.; Cummings, P. T.; Cochran, H. D. *Mol. Phys.* **2003**, *101*, 2157−2169.
(34) Baker, J.; Wolinski, K.; Malagoli, M.; Kinghorn, D.; Wolinski, P.; Magyarfalvi, G.; Saebo, S.; Janowski, T.; Pulay, P. *J. Comput. Chem.* **2009**, *30*, 317−335.
(35) Pulay, P. B., J.; Wolinski, K. *PQS Ab Initio*, version 3.3; Parallel Quantum Solutions: Fayetteville, AR, 2003.
(36) Elliott, J. A. *Device and Materials Modeling in PEM Fuel Cells*; Topics in Applied Physics; Springer: New York, 2009; Vol. *113*, pp 413−436.
(37) Elliott, J. A.; Paddison, S. J. *Phys. Chem. Chem. Phys.* **2007**, *9*, 2602−2618.
(38) Mauritz, K. A.; Moore, R. B. *Chem. Rev.* **2004**, *104*, 4535−4585.
(39) Paddison, S. J. *Ann. Rev. Mater. Res.* **2003**, *33*, 289−319.
(40) Hayes, R. L.; Paddison, S. J.; Tuckerman, M. E. *J. Phys. Chem. B* **2009**, *113*, 16574−16589.
(41) Butrow, A. B.; Buchanan, J. H.; Tevault, D. E. *J. Chem. Eng. Data* **2009**, *54*, 1876−1883.
(42) Giotto, M. V.; Zhang, J. H.; Inglefield, P. T.; Wen, W. Y.; Jones, A. A. *Macromolecules* **2003**, *36*, 4397−4403.
(43) Zerda, A. S.; Lesser, A. J. *J. Appl. Polym. Sci.* **2002**, *84*, 302−309.
(44) Zerda, A. S.; Lesser, A. J. *Polym. Eng. Sci.* **2004**, *44*, 2125−2133.
(45) Calzia, K. J.; Forcum, A.; Lesser, A. J. *J. Appl. Polym. Sci.* **2006**, *102*, 4606−4615.
(46) Lyubartsev, A. P.; Laaksonen, A. *J. Biomol. Struct. Dyn.* **1998**, *16*, 579.
(47) Vishnyakov, A.; Widmalm, G.; Kowalewski, J.; Laaksonen, A. *J. Am. Chem. Soc.* **1999**, *121*, 5403−5412.
(48) Manoj, N. R.; Ratna, D.; Weiss, R. A. *Macromol. Res.* **2004**, *12*, 26−31.
(49) Ohkubo, T.; Kidena, K.; Takimoto, N.; Ohira, A. *J. Mol. Model.* **2012**, *18*, 533−540.
(50) Alam, T. M.; Pearce, C. J.; Jenkins, J. E. *Comput. Theor. Chem.* **2012**, 995.
(51) Pavlov, M.; Siegbahn, P. E. M.; Sandstrom, M. *J. Phys. Chem. A* **1998**, *102*, 219−228.
(52) Schwenk, C. F.; Loeffler, H. H.; Rode, B. M. *J. Chem. Phys.* **2001**, *115*, 10808−10813.
(53) Lee, H. M.; Kim, J.; Lee, S.; Mhin, B. J.; Kim, K. S. *J. Chem. Phys.* **1999**, *111*, 3995−4004.